Wave Packets in Perturbed Rydberg Systems

D. W. Schumacher, B. J. Lyons, and T. F. Gallagher
Department of Physics, University of Virginia, Charlottesville, Virginia 22901
(Received 5 August 1996; revised manuscript received 10 March 1997)

We have excited wave packets in perturbed Rydberg states of barium, an atom with two optically active electrons, and have observed qualitatively different wave packets from those seen in one-electron atoms. In particular, we have found that electron-electron scattering quickly leads to excitation of a doubly excited state and subsequent passage of the population back and forth between different configurations or channels, the quantum analog of two coupled pendula. The experimental results can be successfully described by quantum defect theory. [S0031-9007(97)03329-2]

PACS numbers: 32.80.Rm

Wave packets are formed in any system excited by a short enough pulse, and understanding their dynamics is essential [1]. Wave packets in single configurations, such as one-electron Rydberg wave packets or molecular vibrational wave packets correspond to a one dimensional classical oscillatory motion and are well understood [2–4]. Wave packets in perturbed systems, those exhibiting configuration interaction, correspond to the classical motion of two coupled oscillators. Although there have been related investigations [5], such wave packets have received little attention, in spite of the fact that they play a central role in several contexts such as zero kinetic energy spectroscopy and proposed methods for coherent control of chemical reactions [6,7]. The latter are based on the molecular analog of the energy transfer between coupled classical oscillators [8].

Here we describe the experimental observation of radial wave packets of perturbed Ba Rydberg states, specifically the $6snd\ ^{1,3}D_2$ states perturbed by the $5d7d\ ^1D_2$ state near $n = 26$. Although the configuration interaction only slightly perturbs the regularity of the Rydberg energy levels, it alters the oscillator strengths, with the result that the time dependence of the perturbed radial wave packet bears almost no relation to that of an unperturbed radial wave packet. This dramatic difference is implied by the excitation spectrum and can be understood qualitatively with a simple picture based on the atomic population's passing back and forth between the Rydberg states and the doubly excited perturbing level. This picture can be made quantitative using quantum defect theory (QDT), yielding good agreement with the experimental results. Furthermore, time resolved measurements of the doubly excited population show that the population does indeed flow back and forth between the Rydberg states and the perturber.

The system we have studied is the three channel system shown in Fig. 1. The three channels are the $6snd\ ^1D_2$, $6snd\ ^3D_2$, and $5dnd\ ^1D_2$ channels, although only the $5d7d$ state of the third channel is important. For convenience, we shall refer to these three channels as singlet, triplet, and perturber, respectively. In the absence of configuration interaction the energies of the two unperturbed Rydberg series and the $5d7d$ perturber are shown in Fig. 1(a). When the configuration interaction is included, the $5d7d$ state is inserted into the Rydberg series with the result that the regularity of the Rydberg series is perturbed slightly as shown in Fig. 1(b). Equally important, the energy eigenstates become superpositions of singlet, triplet, and perturber, with the mixing most pronounced near the perturber. Inspecting Fig. 1(b) we can immediately see two of the relevant times for this problem. The Kepler time $\tau_K = 2$ ps is equal to the inverse of the Δn level spacing, and the singlet-triplet time $\tau_{ST} = 9$ ps is equal to the inverse of the singlet-triplet splitting. The final relevant time scale comes from the excitation spectrum of these states, shown in Fig. 1(c). To obtain this spectrum we used two 9 ns dye laser pulses. The first was set to the $6s\ ^1S_0$-$6s6p\ ^1P_1$ transition at 554 nm, and the second was scanned over the $6s6p\ ^1P_1$-$6snd\ ^{1,3}D_2$ transitions near 421 nm, as shown in Fig. 1(d). Instead of having the expected $1/n^3$ intensity dependence the spectrum has a hole with almost vanishing intensity at the perturber. It is an example

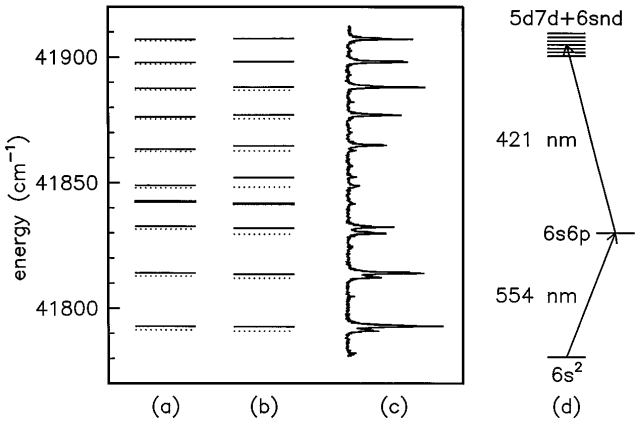

FIG. 1. Barium. (a) Energy levels without configuration mixing derived from QDT: $5d7d\ ^1D_2$ (thick lines), $6snd\ ^1D_2$ (thin lines), $6snd\ ^3D_2$ (dotted lines; (b) actual energy levels; (c) excitation spectrum when exciting via singlet character; (d) excitation pathway from the ground state.

of the Fano $q \approx 0$ line shape [9], and the width of the hole is the inverse of the configuration interaction time $\tau_{CI} = 0.8$ ps. This is the time in which an atom initially in the $5d7d$ state converts, or effectively autoionizes, into the Rydberg states. Note that far from the perturber only the $6snd\ ^1D_2$ states are excited. More generally, the excitation is only to the $6snd\ ^1D_2$ states or their components in perturbed states [10].

Using the well characterized [11] system of Fig. 1 we have used the optical Ramsey method [12] (ORM) to observe perturbed radial wave packets in Ba. The level scheme is shown in Fig. 1(d). Using a 9 ns, 554 nm laser pulse Ba atoms in a thermal beam are excited to the $6s6p\ ^1P_1$ state. From this state they are excited to the perturbed Rydberg states by two 421 nm pulses derived from the second harmonic of an 842 nm, 200 fs Ti: Sapphire laser pulse. The bandwidth of the 421 nm light matches the excitation spectrum of Fig. 1(c). The principle of ORM is to use two identical 421 nm pulses with a variable time delay between them to obtain a wave packet signal which is related to the excitation spectrum of Fig. 1(c) by a Fourier transform. In the frequency domain, changing the time delay between the pulses alters how well the optical power spectrum matches the absorbing atomic states of Fig. 1(c). The time domain provides a more physical picture. In the limit of minimal depopulation of the $6s6p$ state each pulse creates a $6snd\ ^1D_2$ wave packet near the core. If, when the second pulse arrives, the wave packet from the first pulse has returned to the core and is in the singlet states, the two wave packets interfere, constructively or destructively depending on the optical phase, modulating the total number of Rydberg atoms produced. If the first wave packet is elsewhere, there is no interference. We detect the total population of the Rydberg states by field ionization. By measuring the rms amplitude of the interference in the signal as a function of the time delay, we measure the probability of the atoms' being in the singlet Rydberg states near the core as a function of time.

Since the perturbed energy levels of Fig. 1(b) are quite similar to the unperturbed levels of Fig. 1(a), one might expect something like normal radial wave packet behavior with its regular series of fractional revivals [3,4]. However, because of the Fano $q = 0$ excitation spectrum, we observe the result shown by the solid line of Fig. 2(a), which looks nothing like a normal radial wave packet. Furthermore, the three time scales mentioned previously are not particularly evident.

As shown by the dotted line of Fig. 2(a), the major features of the observations are reasonable well reproduced by a QDT model. Before discussing the QDT model it is useful to consider a simple pictorial description. While crude, it does convey the essential notions of the scattering ideas behind the QDT model and describes the behavior, at least for short times. In Fig. 3(a) we show the configuration of the atom just after excitation by a short

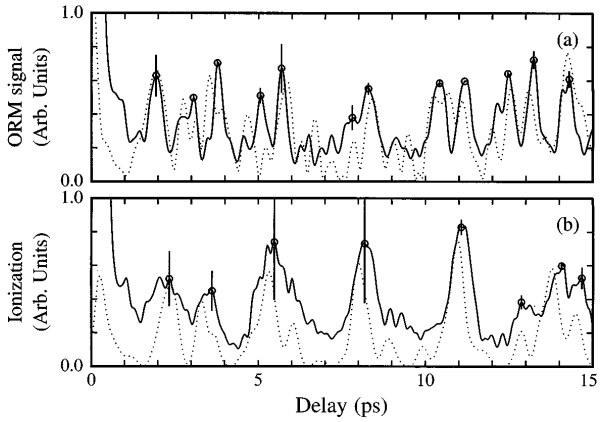

FIG. 2. (a) ORM and (b) ionization signals from a wave packet made of states excited via their singlet character. The data are plotted using solid lines with representative 2σ uncertainties. The model results are shown as dotted lines.

laser pulse. The electron is in the singlet Rydberg states near the core. Half the electrons are incoming and half are outgoing, leading to the creation of two wave packets. To show this, in Fig. 3(a) the atoms are assumed to circulate counter clockwise around the Rydberg orbit. For simplicity, we label the initially outgoing electrons the first wave packet and the initially incoming electrons the second wave packet. While the first wave packet moves out to large radius the second wave packet immediately excites the core and is captured into the $5d7d$ state, as illustrated in Fig. 3(b). Then it is ejected τ_{CI} later, at $t \approx 0.8$ ps, resulting in the double wave packet shown in Fig. 3(c) at $t \approx 1.0$ ps. The first wave packet returns to the core at the Kepler time, at $t \approx 2$ ps [Fig. 3(d)]. It then is captured into the core and again ejected after the configuration interaction time, and the cycle repeats.

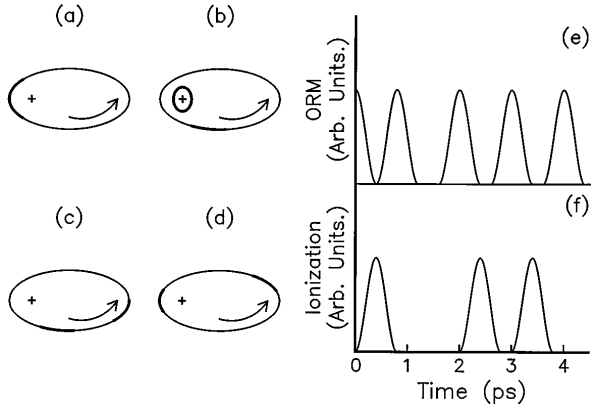

FIG. 3. Schematic of the early evolution of the two-electron wave packet at four consecutive times (a)–(d). Darkened regions on the ellipse represent the locations of singlet wave function. A small, dark ellipse near the nucleus (+) represents the perturber wave function. (e) Expected ORM signal. (f) Expected 5d7d ionization signal.

We expect an ORM signal when the wave packet is in the singlet Rydberg states near the core. This requirement is met at $t = 0$ by both the first and second wave packets and again at $t = 0.8$ ps by the second wave packet. One Kepler time later the first wave packet and then, a configuration time later, the second wave packet are again at the core in a singlet state. The expected signal is shown graphically in Fig. 3(e). Comparing Fig. 3(e) to the experimental signal of Fig. 2(a) we can see that there is qualitative agreement for roughly two Kepler times, after which point the simplicity of our model takes its toll.

Implicit in this simple picture is the notion that the atomic population is passing back and forth between the $5d7d$ state and the $6snd$ Rydberg states, and we can use the same picture to predict when population should be in the $5d7d$ state. There should be a peak in the $5d7d$ population from the second wave packet at $\sim$0.8 ps and a double peak spaced by 0.8 ps every Kepler time thereafter. This double peak should occur between the triple peak of the ORM signal, with the expected signal shown in Fig. 3(f).

To test experimentally that the population is passing back and forth we have taken advantage of the fact that, due to its proximity to the Ba^+ $5d$-$6p$ transition at 650 nm, the $5d7d$ state is far more efficiently photoionized than the $6snd$ states by the 842 nm fundamental Ti:Sapphire light [9]. Light at 495 nm would preferentially ionize the $6snd$ states, especially when the Rydberg electron is at its outer turning point [13]. Such a time resolved projection is central to the notion of coherent control [8], and its application to ionization was suggested by Seel and Domcke [14]. We use a 421 nm second harmonic pulse to create the perturbed wave packet and a delayed 842 nm pulse to provide a time resolved probe of population in the $5d7d$ state. In this case we collect the photoelectrons using a 3 V/cm static field as we scan the delay of the 842 nm laser pulse. This field has no effect on the wave packet's dynamics over the time duration studied, about 15 ps.

The result of this experiment is shown in Fig. 2(b), as well the results of the QDT model. The double peak structure predicted by our simple model is clearly visible for two Kepler times, supporting the validity of the model. An unexpected observation is that in both the experimental results and the QDT model the double peak coalesces into a single peak at about 10 ps. This self focusing of the wave packet into the perturber by the configuration interaction could turn out to be very useful in coherent control applications.

We now describe a QDT model of wave packet evolution in a perturbed system. Henle *et al.* have examined this problem using a different formulation of QDT [15], Vrijen *et al.* have used a discrete state approach [16], and Wang and Cooke have examined the related problem of notched wave packets using QDT [17]. We describe the ith eigenstate of our wave packet as a superposition of singlet, triplet, and perturber wave-functions. Explicitly,

$$\psi_i = A_{si}\phi_{si} + A_{ti}\phi_{ti} + A_{pi}\phi_{pi}, \tag{1}$$

where s, t, and p denote singlet, triplet, and perturber. The ϕ_{ji} are the constituent two-electron wave functions, and A_{ji} are their amplitudes. The amplitudes A_{ji} are derived from the energy levels given in Fig. 1(a) using QDT [17]. All quantities are in atomic units, and we assume state normalization, although energy normalization is more common in QDT treatments.

A wave packet Ψ is simply a superposition of the various eigenstates with amplitudes determined by the excitation

$$\Psi(t) = C\sum_i S_i A_{si}\cos(\pi\nu_{si} + \gamma)\Psi_i . \tag{2}$$

Here, S_i is the laser electric field amplitude at the excitation frequency for state i, and C is a constant of proportionality. The factor A_{si} is present because we are exciting via the state's singlet character, and the cosine term describes the $q = 0$ Fano profile in the excitation probability caused by the presence of the perturber. With $\gamma = 0.2$ the calculated spectrum fits the experimental one of Fig. 1(c). None of the results presented in this work depend critically on γ. In Eq. (2) ν_{si} is the effective quantum number relative to the ionic barium $6s$ limit (42035.04 cm^{-1}) and, for a state with energy E_i relative to the $6s$ limit, is given by $E_i = -1/2\nu_{si}^2$. The square of the factor $A_{si}\cos(\pi\nu_{si} + \gamma)$ is proportional to the cross section for exciting state i. The model is valid only in the weak field regime in which the $6s6p$ launch state is not significantly depleted, so we are free to choose C so that $\Psi^*\Psi$ is normalized to unity. Finally, we can extract the time-dependent variation in the wave packet's character by projecting out a given character from Eq. (2). We find the probability, P_j, that the wave packet will have j character, where $j = s, t, p$, to be

$$P_j(t) = \sum_i \alpha_i^2 A_{ji}^2 + 2\sum_{i,\beta<i}\alpha_i\alpha_\beta A_{ji}A_{j\beta}\langle\phi_{ji}|\phi_{j\beta}\rangle \times \cos\omega_{i\beta}t . \tag{3}$$

Here, $\alpha_i = CS_iA_{si}\cos(\pi\nu_{si} + \gamma)$ contains the excitation terms from Eq. (2), and $\omega_{i\beta}$ is the energy difference between eigenstates. The cosine terms are the sole source of time variation, and they contribute only insofar as the overlap integrals $\langle\phi_{ji}|\phi_{j\beta}\rangle$ are nonzero. In a nonperturbed system, or in this system, but further from the perturber, the effective quantum numbers of nearby eigenstates differ by unity, the overlap integrals are all zero, and there is no character variation in time. In a perturbed system, the nearby energy levels are shifted, the effective quantum numbers differ by noninteger values, and the overlap integrals are nonzero. A simple analytical expression exists for the overlap integral for most cases of interest, alternatively it can be evaluated numerically [13].

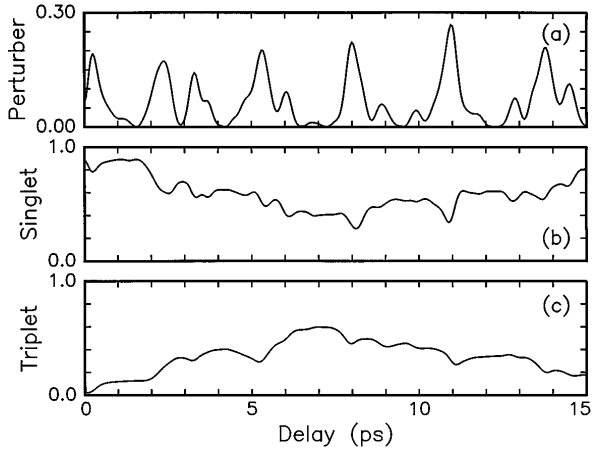

FIG. 4. QDT calculation of perturber (a), singlet (b), and triplet (c) characters versus time after excitation.

Finally, the ORM signal is given by [12]

$$S_{\mathrm{orm}}(t) = \mathrm{RMS}\left[\sum_i \alpha_i(1 + \cos\omega_{i,6s6p}t)\right], \quad (4)$$

where RMS means to take the root-mean-square and $\omega_{i,6s6p}$ is the ith state's energy with respect to the $6s6p$ launch state. As already stated, the model results, Eqs. (3) and (4), are plotted in the Figs. 2(b) and 2(b), and the agreement with experiment is reasonable. Rather than use the ORM as an indicator of the core localized singlet wave function, we can also use Eq. (3) by integrating the overlap integral only over the core. Doing so gives a result similar to Eq. (4), and we shall discuss the point in another paper.

It is illuminating to follow the changing character of the wave packet using the model. Figures 4(a), 4(b), and 4(c) plot the perturber, singlet, and triplet character variation versus time after excitation. The wave packet begins with mostly singlet character. With each sudden dip in the singlet character, we see a burst of perturber, or doubly excited, character with a width given by the configuration interaction time. After decay of the doubly excited state, if the singlet character returns to its previous level (for example, at 0.5 ps), then the scattering simply led to a phase shift. If it does not, then population has scattered into the triplet channel. Although there is no direct coupling between singlet and triplet channels in our model, they still couple via scattering from the doubly excited state. Population is able to pass coherently into the triplet channel until the triplet channel dephases from the singlet channel. The dephasing time is, of course, τ_{ST} described earlier. The perturber bursts grow in height because they are fed first by the singlet channel only, but later by the triplet channel as well.

We have demonstrated that even a perturbation that gives rise to only small energy shifts can have a dramatic effect on wave packet propagation because the population passes back and forth between configurations. The ensuing dynamics can be explained in a very physical way by a QDT model which describes the interaction of the various possible configurations, or channels. This approach should prove to be not only useful, but mandatory, as more complicated systems are explored.

We gratefully acknowledge fruitful discussions with R. R. Jones. This research was supported by the U.S. Department Energy.

[1] R. R. Jones and P. H. Backsbaum, Phys. Rev. Lett. **67**, 3215 (1991); A. Zavriyev, P. H. Backsbaum, J. Squier, and F. Saline, Phys. Rev. Lett. **70**, 1077 (1993); M. P. deBoer *et al.*, Phys. Rev. Lett. **71**, 3263 (1993).
[2] L. S. Brown, Am. J. Phys. **41**, 525 (1973).
[3] A. ten Wolde *et al.*, Phys. Rev. Lett. **61**, 2009 (1988); J. A. Yeazell, M. Mallalieu, J. Parker, and C. R. Stroud, Jr., Phys. Rev. A **40**, 5040 (1989).
[4] I. Sh. Averbukh, and N. F. Perelman, Phys. Lett. A **139**, 449 (1989); M. Nauenberg, J. Phys. B **23**, L385 (1990).
[5] J. G. Story, D. I. Duncan, and T. F. Gallagher, Phys. Rev. Lett. **71**, 3431 (1993); J. H. Hoogenraad, R. B. Vijren, and L. D. Noordam, Phys. Rev. A **50**, 4133 (1994); D. W. Schumacher, D. I. Duncan, R. R. Jones, and T. F. Gallagher, J. Phys. B **29**, L1 (1996).
[6] K. Muller-Dethlefts and E. W. Schlag, Annu. Rev. Phys. Chem. **42**, 109 (1991); I. Fisher, D. M. Villeneuve, M. J. J. Vrakking, and A. Stolow, J. Chem. Phys. **102**, 5566 (1995).
[7] J. J. Gerdy *et al.*, Chem. Phys. Lett. **75**, 3410 (1995); B. Kohler *et al.*, Phys. Rev. Lett. **74**, 3350 (1995).
[8] D. J. Tannor and S. A. Rice, J. Chem. Phys. **83**, 5013 (1985).
[9] U. Fano, Phys. Rev. **124**, 1866 (1961).
[10] O. C. Mullins, Y. Zhu, and T. F. Gallagher, Phys. Rev. A **32**, 243 (1985).
[11] M. Aymar and O. Robaux, J. Phys. B **12**, 531 (1979).
[12] L D. Noordam, D. I. Duncan, and T. F. Gallagher, Phys. Rev. A **45**, 4734 (1992); R. R. Jones, D. W. Schumacher, T. F. Gallagher, and P. H. Bucksbaum, J. Phys. B **28**, L405 (1995).
[13] S. A. Bhatti, C. L. Cromer, and W. E. Cooke, Phys. Rev. A **24**, 161 (1981).
[14] M. Seel and W. Domcke, J. Chem. Phys. **95**, 7806 (1991).
[15] W. A. Henle, H. Ritsch, and P. Zoller, Phys. Rev. A **36**, 683 (1987).
[16] R. B. Vrijen, J. H. Hoogenraad, and L. D. Noordam, Phys. Rev. A **52**, 2279 (1995).
[17] X. Wang and W. E. Cooke, Phys. Lett. **67**, 976 (1991); X. Wang and W. E. Cooke, Phys. Rev. A **46**, R2201 (1992).
[18] T. F. Gallagher, *Rydberg Atoms* (Cambridge University Press, Cambridge, 1994).